Developmental Cell, Vol. 3, 557–568, October, 2002, Copyright ©2002 by Cell Press

Regulated Proteolysis of Xom Mediates Dorsoventral Pattern Formation during Early *Xenopus* Development

Zhenglun Zhu[1,2] and Marc Kirschner[1,3]
[1]Department of Cell Biology
Harvard Medical School
240 Longwood Avenue
Boston, Massachusetts 02115
[2]Division of Gastroenterology
Department of Medicine
Brigham and Women's Hospital
Boston, Massachusetts 02115

Summary

To identify a regulatory role for proteolysis during early *Xenopus* development, we developed a biochemical screen for proteins that are degraded in an embryonic stage-specific manner. We found that Xom, a homeobox transcriptional repressor of dorsal-specific genes, was degraded precipitously during early gastrulation. Xom degradation is regulated by phosphorylation at a GSK3-like consensus site and is most likely mediated by the SCF-β-TRCP complex. Expression of nondegradable Xom represses transcription of dorsal genes much more effectively than wild-type Xom and results in a more strongly ventralized phenotype. We propose that regulated Xom proteolysis plays an essential role in the establishment of the dorsoventral axis, by converting a gradient in BMP abundance into a sharp dorsoventral pattern.

Introduction

Regulated proteolysis mediated by ubiquitin plays an essential role in biological processes such as the cell cycle, transcription, antigen presentation, inflammation, and repair of DNA damage (Hershko and Ciechanover, 1998; Hochstrasser, 1996; Peters et al., 1998). Although each of these processes may be important in embryonic development, little is known about the explicit involvement of regulated proteolysis in differentiation and patterning of the developing embryo.

Two signaling pathways have been especially implicated in patterning of the mesoderm during embryogenesis, the Wnt signaling pathway and the BMP signaling pathway (Harland and Gerhart, 1997; Hoppler and Moon, 1998). The role of proteolysis in development was first suggested by the findings that proteolysis of β-catenin was selectively inhibited on the future dorsal side of the *Xenopus* embryo, which marked the initial step in dorsoventral axiation (Larabell et al., 1997; Miller et al., 1999). The accumulation of β-catenin at the future dorsal side of the embryos (Larabell et al., 1997; Miller et al., 1999) is required for the formation of the Spemann organizer at the dorsal midline, which secretes factors that antagonize Wnt8 and BMP4 signaling, allowing the development of neural structures and the head (De Robertis et al., 2000; Niehrs, 2001).

[3]Correspondence: marc@hms.harvard.edu

To ask more generally whether proteolysis plays a role in early pattern formation after the initial dorsoventral axis determination process, we developed a screen for proteins that are differentially degraded during development. We found that Xom (also known as Vent-2, Vox, and Xbr-1; Ladher et al., 1996; Onichtchouk et al., 1996; Papalopulu and Kintner, 1996; Schmidt et al., 1996), a homeobox transcription factor in the BMP4 signaling pathway, is degraded in an embryonic stage-specific manner. Xom exerts its ventralizing effect by binding to the BIE motif of dorsal-specific genes such as Goosecoid, acting as a direct transcriptional repressor (Trindade et al., 1999). Previous studies showed that the spatial expression pattern of Xom RNA is similar to that of BMP4. Prior to gastrulation (stage 9), Xom is expressed throughout the embryo (Ladher et al., 1996; Schmidt et al., 1996). During early gastrulation (stage 10.5), Xom RNA is located at the ventral lateral regions of the embryo but is absent from the Spemann organizer (Ladher et al., 1996; Onichtchouk et al., 1998; Schmidt et al., 1996). Ectopic expression of Xom on the dorsal side ventralizes the embryo, which resembles the effect of BMP4 overexpression (Ladher et al., 1996). Moreover, the dorsalizing phenotype resulting from ectopic expression of the dominant-negative BMP receptor can be rescued by ectopic expression of Xom (Onichtchouk et al., 1998).

Our current experiments show that the same ubiquitination pathway that mediates the degradation of β-catenin is also involved in the degradation of Xom. As in β-catenin, Xom degradation is controlled by the phosphorylation status of the GSK3-like consensus site in the Xom destruction motif. Xom degradation is activated abruptly at gastrulation. Nondegradable Xom is more active than wild-type in blocking the transcription of the Goosecoid promoter. Ectopic expression of nondegradable mutants of Xom on the dorsal side results in severe disruption of dorsal structure formation. These findings suggest that regulated proteolysis is important not only for the initiation, but also for the later establishment of the dorsoventral axis. We discuss a model by which a temporally initiated process of Xom degradation plays a role in establishing a sharp dorsoventral spatial distribution of BMP; this in turn leads to dorsoventral polarity in gastrulation.

Results

Identification of Xom as a Protein Whose Stability Is Developmentally Regulated

Xenopus egg extracts have been used extensively to study regulation of the cell cycle (Murray, 1991). When combined with screening of proteins synthesized from small pools of cDNAs, it has successfully identified proteins that are differentially phosphorylated or degraded at different phases of the cell cycle (Lustig et al., 1997; McGarry and Kirschner, 1998; Stukenberg et al., 1997;

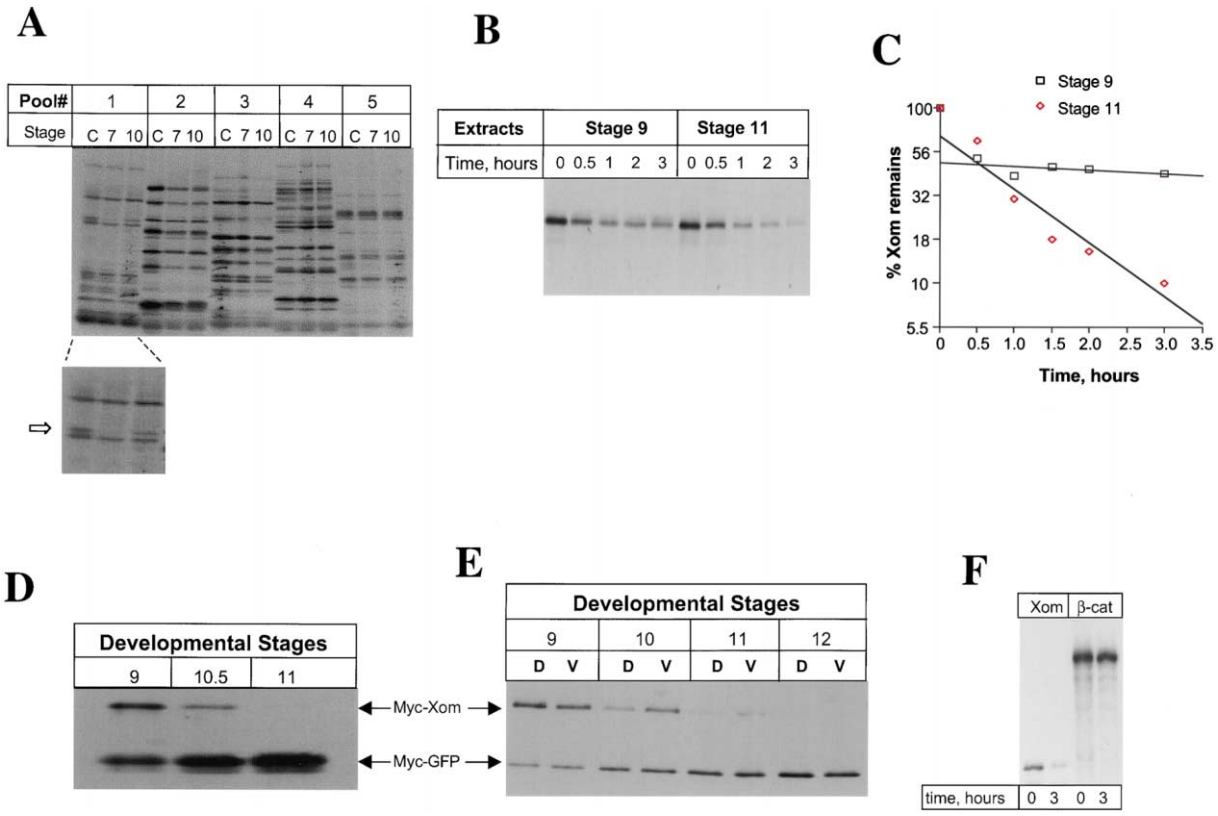

Figure 1. Identification of Xom as a Protein Whose Stability Is Developmentally Regulated

(A) cDNAs from small pools of 50–100 plasmids were transcribed and translated in vitro in the presence of [^{35}S]methionine as described in the text. The ^{35}S-labeled proteins were incubated with either pre-MBT extract (stage 7) or post-MBT extract (stage 10) for 3 hr at room temperature; the proteins were separated on SDS-PAGE and revealed by autoradiography. As shown in pool #1, a band, later shown to be Xom, is degraded by the pre-MBT extract but not by the post-MBT extract, as indicated by the arrow.

(B) ^{35}S-labeled Xom was incubated with either stage 9 or stage 11 extracts for 3 hr and degradation kinetics were followed as indicated.

(C) The kinetics of Xom degradation in stage 9 and stage 11 extracts plotted on a log scale. The first-order rate constant for degradation coefficiency was calculated using data between 30 and 180 min.

(D) mRNA (0.4 ng) encoding myc-tagged Xom was injected into two blastomeres at the two-cell stage. mRNA (0.1 ng) encoding myc-tagged GFP was coinjected as an internal loading control. The embryos were allowed to develop until the stages indicated, and the amount of myc-Xom was detected by Western blot as described.

(E) mRNAs encoding myc-Xom and myc-GFP were injected into either the two dorsal blastomeres or the two ventral blastomeres at the four-cell stage. The embryos were allowed to develop until the stages indicated and the amounts of Xom and GFP were assayed as described.

(F) In vitro degradation of Xom and β-catenin in stage 11 extracts.

Zou et al., 1999). More recently, both egg and later embryonic extracts were used successfully to follow β-catenin degradation and recapitulate events of Wnt signaling during early embryogenesis (Salic et al., 2000). To identify the possible functions of proteolysis during early embryogenesis, we utilized these later embryonic extracts to identify proteins degraded in a stage-specific manner. As the midblastula transition (MBT) marks an important developmental stage when zygotic transcription, cell migration, and a more complex cell cycle begin (Newport and Kirschner, 1982), we asked whether there were proteins that were differentially degraded before and after that transition, as is the case for cyclin E (Howe and Newport, 1996). As shown in Figure 1A, in the screening experiments, small pools of 50–100 cDNAs were transcribed and translated in reticulocyte extract and labeled with [^{35}S]methionine. After incubation in pre- (stage 7.5–8) or post- (stage 10–10.5) MBT extracts for 3 hr, the proteins were separated by SDS-PAGE and the autoradiographs were compared. In 900 small pools of *Xenopus* blastula and neurula cDNAs, we identified two small pools that contained proteins that were degraded more rapidly by the pre-MBT extract. After subsequent sib selection and cloning, the gene encoding one of the unstable proteins was identified as Xom; the other did not correspond to known protein in the database.

The Timing of Xom Degradation

At gastrula stages, the expression pattern of Xom mRNA is similar to that of BMP4 and complementary to that of the dorsal marker Xnot (Ladher et al., 1996; Onichtchouk et al., 1996; Papalopulu and Kintner, 1996; Schmidt et al., 1996). The finding that Xom protein is unstable in pre-MBT extracts and stable in gastrula extracts suggested that the Xom protein level may be under specific developmental regulation, especially later in gastrulation when Xom is expressed. We therefore further examined the biochemical properties of Xom degradation during early development both in vitro and in vivo. For the in vitro experiments, [^{35}S]methionine-labeled Xom was

incubated in embryonic extracts prepared from either stage 9 or 11. The degradation kinetics of Xom in different gastrula extracts was followed on SDS-PAGE. As shown in Figure 1B, Xom was degraded more rapidly in extracts of stage 11 embryos, but remained stable in extracts from stage 9. As shown in Figure 1C, the degradation rate of Xom in stage 9 extracts was nearly zero (0.023 hr^{-1}), or a half-life of 30 hr. In stage 11 extracts, the rate is 13 times faster (0.31 hr^{-1}), or a half-life of 2.2 hr. The stage-specific degradation of Xom indicates that the proteolysis process is developmentally regulated. The rate of Xom degradation is decreased in embryos that have been ventralized by UV irradiation at the one-cell stage (data not shown), further suggesting developmental regulation. Proteolysis of Xom was also shown to be very specific. As illustrated in Figure 1F, when incubated with stage 11 extracts, Xom was rapidly degraded, whereas β-catenin remained stable. The differential degradation of Xom and β-catenin in the staged extracts again indicates that proteolysis of Xom and β-catenin are both regulated processes.

For in vivo experiments, mRNA encoding myc-tagged Xom was injected in both blastomeres at the two-cell stage, the embryos were cultured to the stages indicated, and the amount of Xom protein was determined. Coinjected myc-tagged GFP was used as an internal control. As shown in Figure 1D, Xom disappears rapidly after stage 10–10.5, while the myc-GFP shows a small increase during the same period. Changes in Xom protein level could reflect changes in proteolysis, changes in translational initiation, or changes in RNA level. Since both myc-tagged GFP and myc-tagged Xom were in the same vector with identical 5′ and 3′ sequences, the level of translation initiation of both proteins should be the same. A single point mutation in the Xom coding region stabilizes Xom protein in vivo (see Figure 3D); therefore, it is unlikely that the disappearance of Xom protein is due to RNA instability or different rates of protein synthesis. Therefore, changes in the Xom protein level during the early gastrulation stage most likely reflect changes in the rate of proteolysis. We also examined Xom degradation separately in dorsal and ventral hemispheres by injecting mRNA encoding Xom into either the two dorsal or the two ventral hemispheres at the four-cell stage. As shown in Figure 1E, Xom disappears from both the dorsal side and the ventral side by stage 12. However at stages 10 and 11, there is a slightly greater loss of Xom at the dorsal side. We observed decreased levels of Xom on the dorsal side at stage 10 in six out of ten experiments; we never observed greater levels on the dorsal side.

The Mechanism of Xom Degradation

Xom is degraded by the ubiquitin/proteosome pathway, as shown in Figure 2A. When ^{35}S-labeled Xom was incubated in extracts from stage 11 in the presence of His-ubiquitin, polyubiquitinated Xom of high molecular weight was recovered from Ni beads, indicating polyubiquitination. We also examined the stability of Xom in the presence of proteosome inhibitors. As shown in Figure 2B, clasto-lactocystin-β-lactone (an irreversible proteosome inhibitor; Fenteany et al., 1995) at a concentration of 100 μM efficiently blocked the degradation of Xom; the minimal effective concentration in extract was about 25–50 μM (data not shown).

To search for sequence features required for Xom degradation, we constructed a series of deletion mutants and assayed their stability in staged extracts (data not shown). A region between amino acids 132 and 154 is required for the stability of Xom, as shown in Figures 2C and 2D. Xom contains two PEST domains (regions of peptide enriched in proline, aspartic and glutamic acids, serine, or threonine residues; Peters et al., 1998). The first PEST domain of Xom is located near the amino terminus (amino acids 29–86), and when deleted, has no effect on stability (data not shown). The sequence 132–154 of Xom corresponds to part of the second PEST domain (amino acids 131–172; Figure 2C), and when deleted (XomΔ20), Xom is stabilized; we refer to this region as the Xom destruction motif. We showed that XomΔ20 migrates as a higher molecular weight species after incubation with stage 11 extract (Figure 2D), indicating that XomΔ20 was phosphorylated outside the destruction motif. We went on to test the stability of XomΔ20 in vivo. mRNAs encoding myc-tagged XomΔ20 or wild-type Xom were injected into either two dorsal or two ventral blastomeres at the four-cell stage. The amount of Xom at each developmental stage was measured by Western blot. As shown in Figure 2E, the Xom protein encoded by XomΔ20 remains stable in both the dorsal and ventral regions of the embryo. In contrast, wild-type Xom was cleared completely from both regions before stage 11.

A GSK3-like Consensus Phosphorylation Site in the Xom Destruction Motif Is Necessary for Xom Degradation

Previous studies indicated that PEST domains may provide recognition sequences for phosphorylation, which could provide regulated signals for degradation (Lanker et al., 1996; Yaglom et al., 1995). Such signals regulate the degradation of vertebrate transcription factors, such as β-catenin and IKBα (Chen et al., 1998; Yost et al., 1996). We therefore looked for potential phosphorylation sites associated with the 132–154 region of Xom that might be important for degradation. We made several constructs that converted single or several serine/threonine residues of the Xom destruction motif into alanine (Figure 3A). The stability of Xom proteins encoded by these mutant constructs was tested in vitro. As shown in Figure 3B, when serine 140 or 144 was converted to alanine, Xom was partially stabilized in stage 11 extracts. The degradation kinetics of wild-type Xom and the Xom S140A, S144A double mutant (Xom2sa) were followed in the same set of experiments as in Figure 1C. After initial rapid loss of the in vitro translated protein, Xom2sa remained stable during the incubation (κ = 0.019 hr^{-1}, or a half-life of 36 hr), while as shown in Figure 1C, the wild-type Xom was completely degraded after 3 hr of incubation (κ = 0.31 hr^{-1}, or a half-life of 2.2 hr). Wild-type Xom is degraded about 16 times faster than the Xom2sa mutant. The initial rapid loss of labeled protein followed by slow degradation appears to be the property of several in vitro translated proteins in the extracts, and is not Xom specific. Virtually all in vitro translated proteins, including GFP, show partial rapid degradation in extracts, a process most likely mediated by nonspecific proteases rather than the proteosome, since the initial loss cannot be blocked by specific proteosome inhibitors (data not shown). After the first few

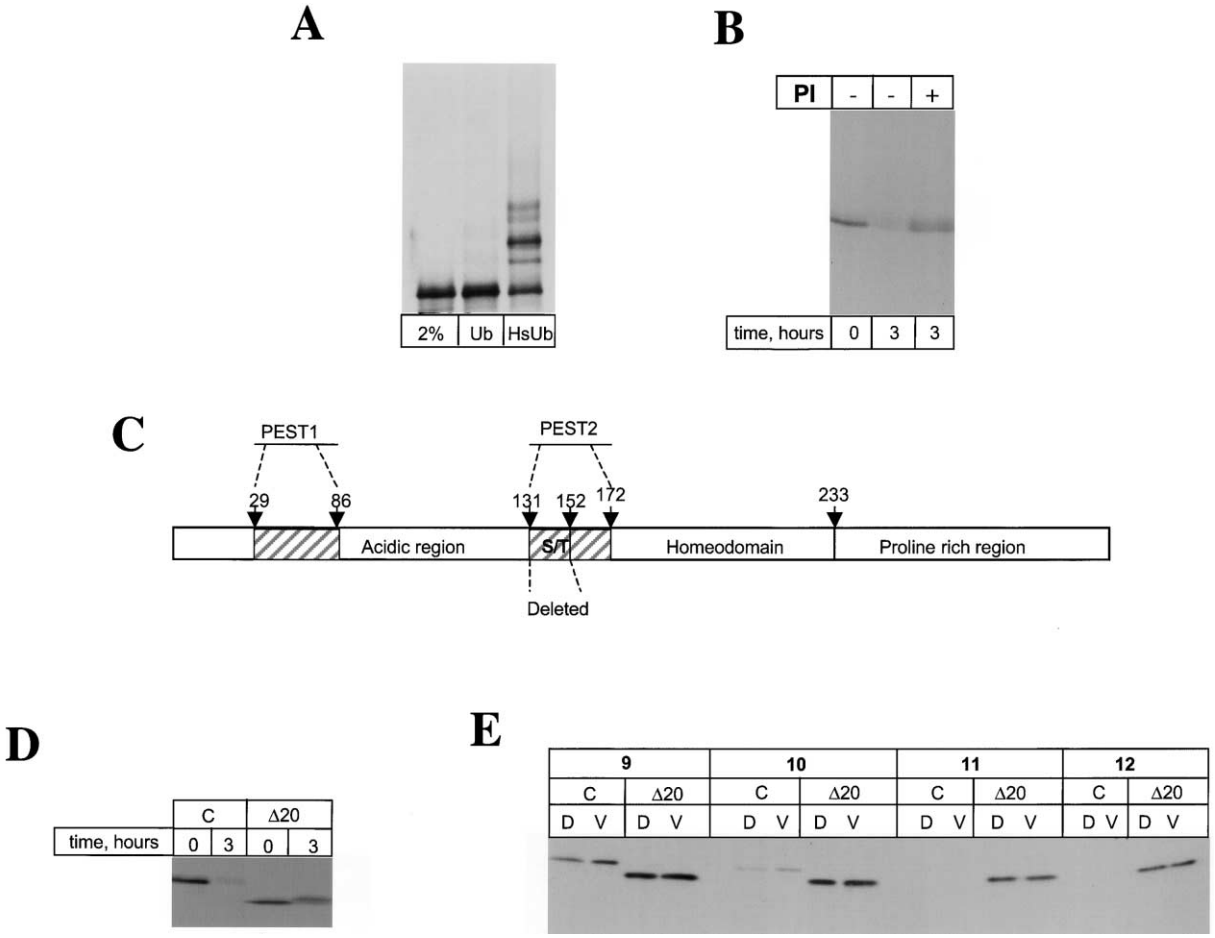

Figure 2. Xom Is Degraded by a Ubiquitin-Mediated Pathway

(A) ^{35}S-labeled Xom was incubated with high-speed stage 11 extracts in the presence of his-tagged ubiquitin (HsUb) or ubiquitin (Ub). Polyubiquitinated Xom was identified after binding to nickel beads and elution. A 2% loading control of labeled Xom protein was included.

(B) ^{35}S-labeled Xom was incubated with stage 11 extract in the presence (+) or absence (−) of 100 μM clasto-lactocystin-β-lactone (PI) for 3 hr at room temperature.

(C) Schematic structure of Xom. The amino acid sequence from 132 to 154 was deleted to create the deletion mutant of Xom, XomΔ20.

(D) ^{35}S-labeled Xom and XomΔ20 were incubated with stage 11 extract at room temperature for 3 hr, and the proteins were analyzed by SDS-PAGE and autoradiography.

(E) mRNA (0.4 ng) encoding either myc-tagged Xom or myc-tagged XomΔ20 was injected into either the two dorsal blastomeres (D) or the two ventral blastomeres (V) at the four-cell stage. The embryos were allowed to develop to the stages indicated and the amount of remaining Xom protein was determined by Western blotting.

minutes, the degradation of the remaining Xom and other proteins showed first-order kinetics. The stability of Xom2sa was also tested by an in vivo assay using the myc-tagged form of the protein. As shown in Figure 3D, the protein level of the Xom2sa mutant remains high in both the dorsal and ventral sides of the embryos at stages 11 and 12, while the wild-type Xom protein cannot be detected after stage 11 on either side.

The sequence DSGYES of the Xom destruction motif, containing serines 140 and 144, resembles the GSK3 consensus phosphorylation site DSGXXS, which is important for stability and is conserved in β-catenin and IKBα and human immunodeficiency virus (HIV)-1 protein Vpu (Laney and Hochstrasser, 1999; Maniatis, 1999). To further test the importance of the phosphorylation of the GSK3-like consensus phosphorylation site in the degradation of Xom, we tried to block Xom degradation with the 20-amino acid peptide that corresponds to the Xom destruction motif. As shown in Figure 3E, a peptide that contains phosphoserines at positions 140 and 144 blocked Xom degradation in a concentration-dependent manner, whereas a control peptide of similar length but unrelated sequence (from the Xom amino-terminal region) failed to protect Xom from degradation. The importance of phosphorylation of the GSK3-like consensus phosphorylation sites in the degradation of Xom is further illustrated in Figure 3F. When we attempted to use a native unphosphorylated peptide as a control in this in vitro degradation experiment, paradoxically, the unphosphorylated peptide blocked Xom degradation as effectively as the phosphorylated peptide (Figure 3F, line 2s). However, the same peptide in which serines 140 and 144 were converted into alanines was unable to block Xom degradation by the embryonic extract (Figure

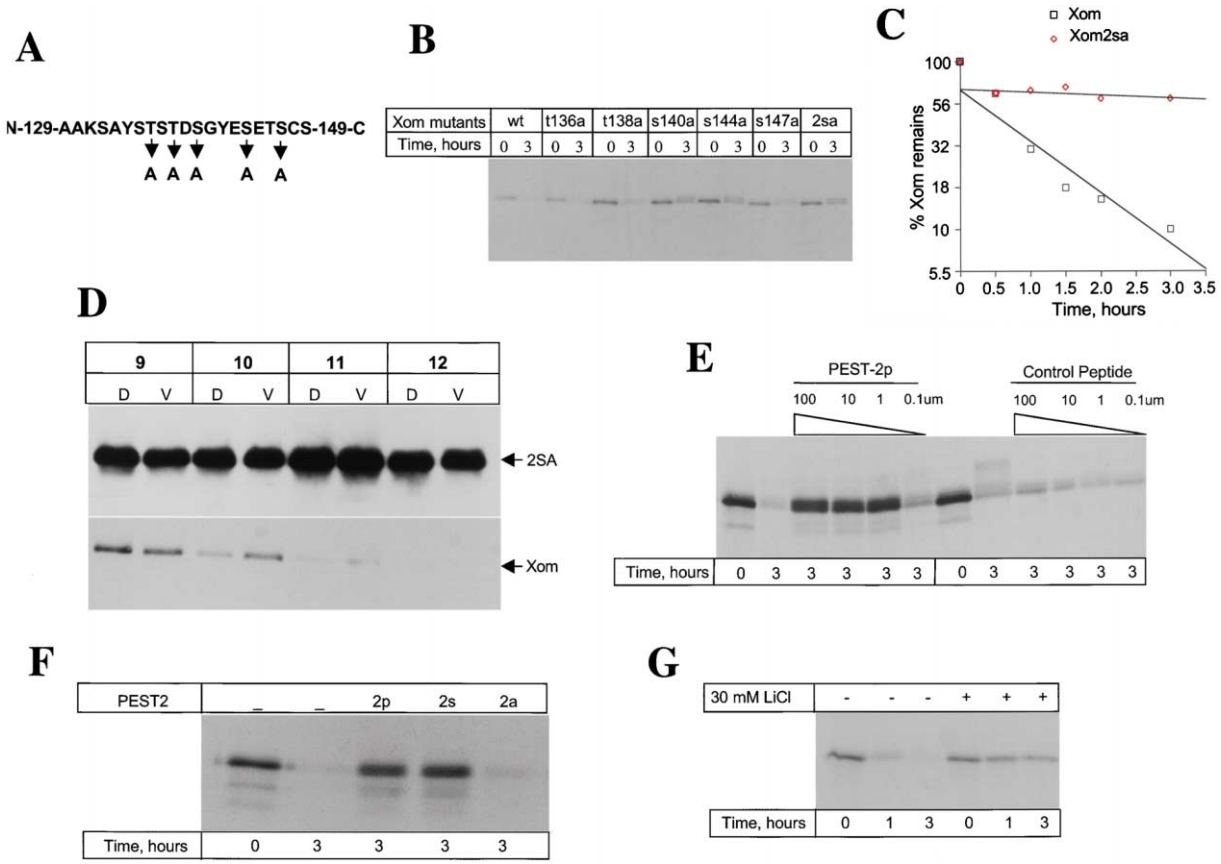

Figure 3. A GSK3-like Consensus Phosphorylation Site Is Important for Xom Degradation

(A) Schematic presentation of serine/threonine-to-alanine mutations of the Xom destruction motif.

(B) In vitro degradation of Xom mutants which contain either single or double serine/threonine to alanine mutations at the indicated positions.

(C) The degradation kinetics of Xom2sa mutant in stage 11 extracts. Data for wild-type control were reproduced from Figure 1C. To calculate the first-order rate constant, data from 30 to 180 min were used. The amount of protein is plotted on a log scale.

(D) In vivo stability of Xom2sa and wild-type Xom at different developmental stages.

(E) [^{35}S]methionine-labeled Xom was incubated with stage 11 extract in the presence of a synthetic peptide corresponding to the Xom destruction motif that contains double phosphoserines at positions 140 and 144 (PEST-2p), or a control peptide of similar length of the Xom amino-terminal sequence. After 3 hr of incubation at room temperature, the amount of Xom proteins remaining was determined.

(F) In vitro degradation of [^{35}S]methionine-labeled Xom in the presence of 10 μM synthetic peptide corresponding to the Xom destruction motif, which contains either two serines (2s), two phosphoserines (2p), or two alanines (2a) at positions 140 and 144.

(G) [^{35}S]methionine-labeled Xom was incubated with stage 11 extract in the presence (+) or absence (−) of lithium for 3 hr at room temperature. The effect of lithium on Xom degradation was revealed by SDS-PAGE and autoradiography.

3F, line 2a). These findings suggest that the embryonic extracts had an enzymatic activity that could phosphorylate serines at positions 140 and 144 in the peptide. Such an activity would be unable to phosphorylate the alanine mutants. The competition between Xom and the native peptide for the kinase in the extracts and phosphorylation of the destruction motif of the native peptide by the embryonic extracts may account for the blocking of Xom degradation by the native peptide but not the nonphosphorylatable peptide.

Xom Degradation Is Regulated by the GSK3-Independent Pathway

We first tested the possible involvement of GSK3 in the regulation of Xom degradation. Xom is stabilized in extracts that contain 30 mM lithium, a rather nonspecific GSK3 inhibitor (Klein and Melton, 1996), as shown in Figure 3G. To focus more specifically on GSK3, we tested the stability of Xom in embryonic extracts depleted of GSK3. GSK3 was depleted by more than 95% by beads coupled to GSK3 binding protein (Salic et al., 2000). Yet under these circumstances, Xom was degraded as efficiently as in undepleted extracts (data not shown). Therefore, we believe that lithium must block Xom degradation by inhibiting a kinase other than GSK3.

Phosphorylation of the GSK3-like Consensus Phosphorylation Site of the Xom Destruction Motif Serves as a Signal for Xom Ubiquitination

To ask whether there was a direct link between Xom ubiquitination and phosphorylation of the Xom GSK3-like consensus site, we measured ubiquitination in vitro, using either the wild-type Xom or the mutant Xom2sa. As shown in Figure 4, after 1 hr of incubation with stage

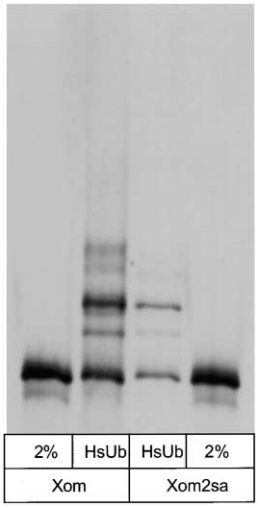

Figure 4. Ubiquitination of Xom and Xom2sa

^{35}S-labeled Xom or Xom2sa were incubated with high-speed stage 11 extract in the presence of his-tagged ubiquitin (HsUb). Polyubiquitinated Xom was identified after binding to nickel beads and elution. A 2% loading control of labeled Xom or Xom2sa protein was included.

11 extracts, polyubiquitinated Xom containing His-tagged ubiquitin was readily detectable from the eluate of Ni beads. By contrast, a lower level of polyubiquitinated species was formed under the same conditions when Xom2sa was used as a substrate for the ubiquitination assay. This experiment suggests that the phosphorylation of the Xom GSK3-like consensus motif is required for ubiquitination of the protein.

SCF-β-TRCP Ubiquitin Ligase Associates Specifically with the Phosphorylated Xom Destruction Motif

The SCF-β-TRCP complex mediates phosphorylation-dependent degradation of several important molecules such as β-catenin and IKBα (Liu et al., 1999; Yaron et al., 1998). Recently, SCF-β-TRCP was found to bind to the phosphorylated destruction motif of β-catenin and IKBα, which contains phosphorylated serine in a GSK3 consensus sequence (Winston et al., 1999). To find whether the SCF complex is associated with the Xom destruction motif, short peptides of 20 amino acids corresponding to the Xom destruction motif were synthesized in either a doubly phosphorylated form (at serines 140 and 144) or a nonphosphorylated form and coupled to agarose beads. The peptide beads were incubated with stage 9.5 and 10.5 extracts. After extensive washing, proteins associated with the beads were eluted with sample buffer, and the presence of the SCF complex was detected by anti-Skp1 immunoblotting. As shown in Figure 5A, Skp1 was readily detected from eluates associated with the phosphorylated Xom destruction motif in both stage 9.5 and 10.5 extracts, but was not detectable from eluates associated with the nonphosphorylated Xom destruction motif. The binding of Skp1 to the phosphorylated Xom motif appears to be indirect. When [^{35}S]methionine-labeled Skp1 was incubated with the phosphorylated destruction motif of Xom, no Skp1 was found to bind to the motif (Figure 5B), suggesting the binding of Skp1 to the Xom destruction motif is most likely mediated by other proteins, notably the F box proteins, which function as substrate receptors for the SCF complex (Skowyra et al., 1997). To search for the F box proteins that might mediate the binding of Skp1 to the destruction motif of Xom, we incubated [^{35}S]methionine-labeled F box proteins of mouse and human origin with affinity beads containing either the phosphorylated Xom destruction motif or the nonphosphorylated Xom destruction motif. As shown in Figure 5C, the human β-TRCP 1a and 1b bound specifically to the phosphorylated destruction motif of Xom. The association of human β-TRCP to the Xom destruction motif is F box independent since the F box-deleted mutant of human β-TRCP 1a (β-TRCP1aΔF) also binds to the Xom destruction motif (although not as strongly as full-length β-TRCP). The binding of human β-TRCP to the phosphorylated Xom destruction motif is probably specific, since other F box proteins, such as hFBW5, mFBX5, and mFBX8, did not bind to the Xom destruction motif under the same conditions (Figure 5C).

β-TRCP Controls Xom Abundance In Vivo

To further investigate the involvement of SCF-β-TRCP in the degradation of Xom, we assayed the effect of hβ-TRCP1aΔF (which may function as a dominant negative) on the stability of Xom during early gastrulation. As shown in Figure 5D, when 0.4 ng mRNA encoding β-TRCP1aΔF was coinjected with 0.4 ng mRNA encoding myc-tagged Xom into both blastomeres at the two-cell stage, the level of Xom protein was increased 5-fold during gastrulation (stage 10). The effect of β-TRCP1aΔF on Xom degradation is similar to its effect on β-catenin degradation (Liu et al., 1999). In contrast to the blocking of Xom degradation by the β-TRCP1aΔF, expression of β-TRCP1a at low concentration increased Xom degradation and lowered the level of Xom. The effect of β-TRCP on the Xom protein level could either be direct or indirect. However, since β-TRCP binds directly to the phosphorylated destruction motif of Xom, it most likely modulates the level of Xom protein during development.

Nondegradable Xom Is More Active Than Wild-Type Xom in Suppressing the Transcriptional Activation of the Goosecoid Promoter by Activin

Previous studies showed that Xom binds to the Goosecoid promoter and suppresses its transcriptional activation by activin (Trindade et al., 1999). To determine whether the nondegradable mutants of Xom also inhibit transcriptional activation by activin, a reporter plasmid containing the Goosecoid promoter of 1500 base pairs fused to luciferase was coinjected with mRNAs encoding either wild-type Xom or nondegradable Xom into two blastomeres at the two-cell stage, along with activin mRNA. After culturing the embryos to stage 10–10.5, the activity of the Goosecoid promoter was measured by a luciferase assay (Watabe et al., 1995). Embryos injected with the reporter and activin mRNA but not Xom served as a control. As shown in Figure 6A, both wild-type Xom and the nondegradable Xom inhibit Goosecoid activation by 80% at an RNA amount of 500 pg. However, below 50 pg, wild-type Xom does not block

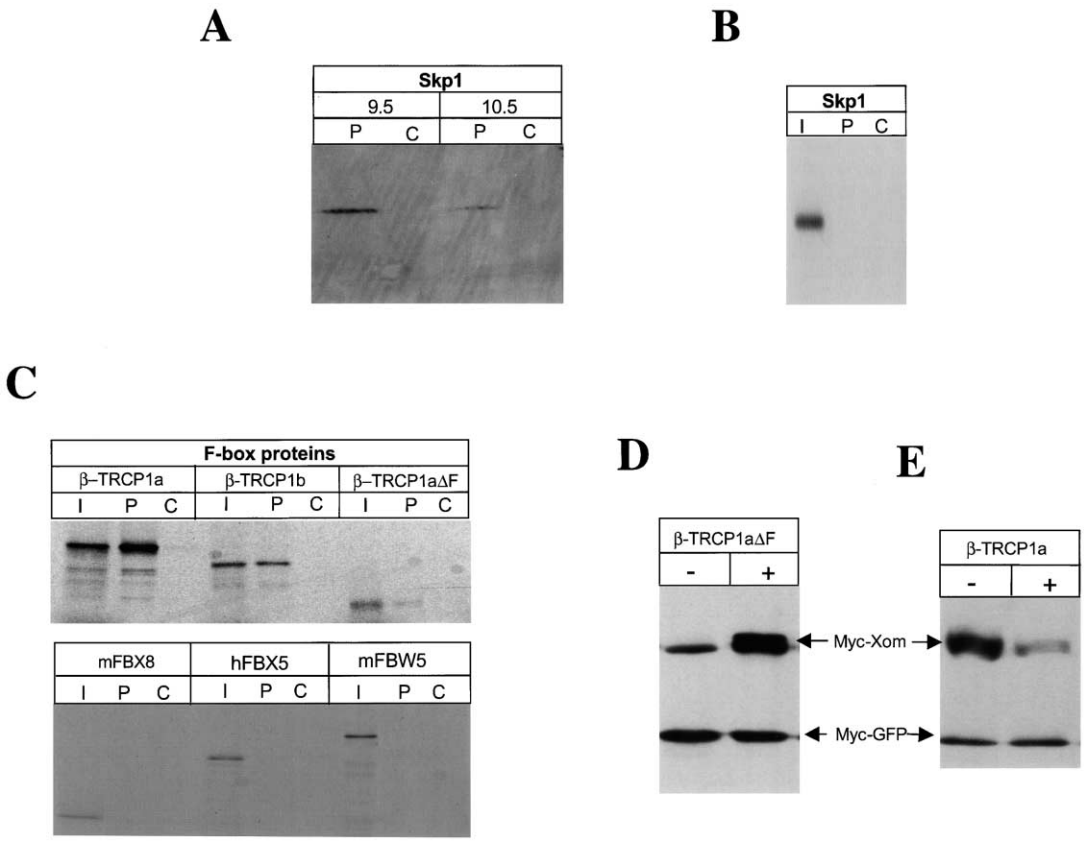

Figure 5. SCF-β-TRCP Binds to the Xom Destruction Motif and Modulates Xom Protein Level In Vivo

(A) Agarose beads containing either the 140, 144 double phosphoserine Xom destruction motif (P), or the wild-type Xom destruction motif (C) were incubated with diluted embryonic stage 9.5 and 10.5 extracts at 4°C for 4 hr. After extensive washing, bound proteins were eluted with sample buffer and applied to SDS-PAGE and subjected to Western blotting using an antibody to Skp1.

(B) ^{35}S-labeled Skp1 was incubated with peptide beads as in (A).

(C) [^{35}S]methionine-labeled β-TRCP 1a, 1b, and 1aΔF (F box-deleted mutant of 1a) and control F box proteins were mixed with the affinity beads as described above. Bound materials were revealed by SDS-PAGE and autoradiography. I: 10% of input control.

(D) mRNA (0.4 ng) encoding myc-Xom was injected into each blastomere at the two-cell stage in either the presence or absence of 0.4 ng of mRNA encoding β-TRCP1aΔF. The embryos were allowed to develop until stage 10 and the amount of Xom was determined by immunoblot using anti-myc antibody as described.

(E) mRNA (2 ng) encoding myc-Xom was coinjected with 0.2 ng mRNA encoding β-TRCP. The embryos were allowed to develop until stage 10 and the amount of Xom was determined as described above.

the Goosecoid promoter, while the nondegradable Xom (Xom2sa) shows inhibition down to 5 pg.

Ectopic Expression of Nondegradable Xom at the Dorsal Side of Embryos Results in an Enhanced Ventralized Phenotype during Embryogenesis

BMP4, a strong ventralizing factor (Graff, 1997; Graff et al., 1994), exerts its effect in part by inhibiting the response to dorsal mesoderm-inducing factors such as activin. Xom was proposed as one of the mediators of the BMP4 effect. The observation that Xom is an unstable protein indicates that proteolysis may serve to limit the repression by Xom on dorsal-specific promoters during early gastrulation. To test the importance of this mechanism, RNA (0.4 ng) encoding the stable XomΔ20 or wild-type Xom was injected into the two dorsal blastomeres at the four-cell stage. The embryos were allowed to develop to tailbud stage. As shown in Figure 6C, expression of the XomΔ20 results in severe head truncation during embryogenesis. Although overexpression of wild-type Xom in dorsal blastomeres also resulted in head truncation in some embryos, the concentration requirement for wild-type Xom to achieve such a phenotype is about 10–20 times that of nondegradable Xom, as shown in Figure 6B. The increased potency of nondegradable Xom in causing head truncation is consistent with its increased potency in suppressing transcription activation of the Goosecoid promoter by activin. Moreover, the effect of nondegradable Xom on dorsal development proved to be spatially restricted. As shown in Figure 6D, when RNA (0.4 ng) encoding XomΔ20 was injected into two ventral blastomeres at the four-cell stage, there was little effect.

Discussion

Although protein degradation had been postulated for more than 50 years to play a central role in overall protein

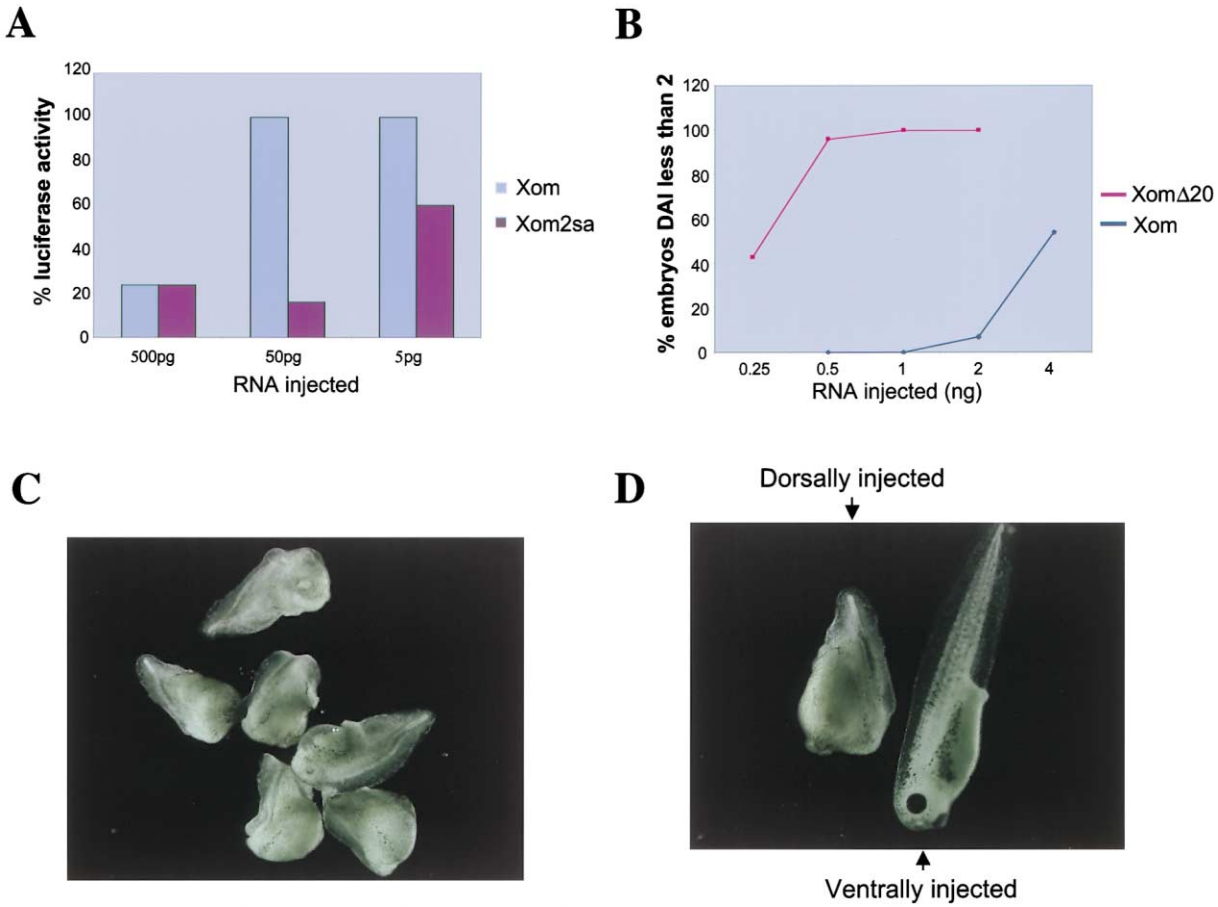

Figure 6. Nondegradable Xom Is More Potent Than Wild-Type Xom in Blocking Goosecoid Promoter Activation and in Ventralizing Embryos

(A) mRNA encoding either wild-type Xom or Xom2sa was injected into both blastomeres at the two-cell stage together with activin RNA (50 pg) and a Goosecoid-luciferase reporter plasmid (100 pg). The embryos were cultured to stage 10.5 and the level of luciferase activity was measured as described.

(B) mRNA encoding Xom or XomΔ20 was injected into both dorsal blastomeres at the four-cell stage. The embryos were cultivated to tailbud stage and the effect of the ectopic expression of nondegradable Xom on development was revealed. The ordinate is a scale of dorsoanterior index (DAI) reflecting the extent of dorsal development, with 5 being a normal embryo, 2 being microcephalic, and 0 being completely ventralized (Kao and Elinson, 1988).

(C) Embryos at the equivalent of tailbud stage, after being injected with 0.4 ng XomΔ20 RNA into both dorsal blastomeres at the four-cell stage.

(D) mRNA (0.4 ng) encoding XomΔ20 was injected into either the two dorsal blastomeres (left embryo) or the two ventral blastomeres (right embryo) at the four-cell stage. The embryos were allowed to develop until the tailbud stage, and the effect of ectopic expression of the nondegradable Xom was revealed.

metabolism (Kirschner, 1999), it is only rather recently that its importance as a key regulator of the cell cycle, inflammation, and transcription has been described. Fundamental to this understanding has been the identification of key substrates of these processes, such as G1 and M phase cyclins as well as p53, IKBα, GCN4, and β-catenin, among others. In all these cases, proteolytic pathways occupy central control points. We have previously shown that in vitro expression cloning using small pools of cDNAs can be used to identify novel targets of regulated degradation in the cell cycle, such as geminin (McGarry and Kirschner, 1998) and securin (Zou et al., 1999). We have applied this screening approach to ask whether there is evidence for stage-specific protein degradation in early embryonic development, and whether it plays a central regulatory role in development.

Identification of Xom as a Developmental Gene Regulated by Proteolysis

We initially targeted our screen to identify genes that are differentially degraded before and after the onset of midblastula transition (MBT). Of more than 50,000 proteins screened (representing an unknown number of different genes), only two were identified clearly to show stage-specific degradation. One was isolated and shown by DNA sequencing to be identical to Xom. The other did not correspond to any known protein in the database. The significance of Xom proteolysis in the pre-MBT extract is not clear, since Xom is not expressed. However, the differential stability of Xom pre- and post-MBT led us to investigate Xom stability throughout gastrulation. We found that Xom is stable during early gastrulation but is degraded at late gastrulation, indicating that proteolysis plays a regulatory role.

Xom Is Degraded by the Ubiquitin-Mediated Pathway during Early Gastrulation

High molecular weight species of Xom conjugated to ubiquitin were found in in vitro assays, and degradation of Xom was blocked by 26S proteosome inhibitors, indicating that Xom is degraded by the ubiquitin-proteosome pathway. We found that part of the second PEST domain of Xom is crucial to conferring instability to the Xom protein. This domain contains a GSK3-like consensus phosphorylation sequence, DSGXXS (Yost et al., 1996), which has been shown to be important in the degradation of β-catenin, IKBα, and HIV-1 protein Vpu/CD4 (Laney and Hochstrasser, 1999; Maniatis, 1999). Mutagenesis studies and the peptide blocking experiments showed that the phosphorylation status of the two serines in the GSK3-like consensus site is important for the degradation of Xom, and that the phosphorylation of the GSK3-like consensus sequence provides a signal for Xom ubiquitination and subsequent degradation. Since both serines are shown to be important, a question remains whether these sites are phosphorylated simultaneously or sequentially, as in the case of sic 1 degradation (Deshaies and Ferrell, 2001; Nash et al., 2001). In searching for the kinases involved in Xom degradation, we have shown that Xom degradation is not triggered by GSK3. Interestingly, of the three proteins that bear GSK3-like consensus phosphorylation sites, only β-catenin is actively phosphorylated by GSK3; IKBα is phosphorylated by the IKB kinase complex (Zandi et al., 1998) and the HIV-1 protein Vpu is phosphorylated by casein kinase II (Paul and Jabbar, 1997; Schubert et al., 1994).

The ubiquitin ligase involved in Xom ubiquitination is likely to be β-TRCP, the E3 complex that mediates the degradation of β-catenin and IKBα (Maniatis, 1999). β-TRCP binds to the phosphorylated destruction motif of Xom, as it does to the phosphorylated destruction motifs of β-catenin and IKBα. In support of this conclusion, the F box-deleted mutant of β-TRCP blocks Xom degradation in vivo, and low concentrations of wild-type β-TRCP increase the rate of degradation of Xom in vivo. However, we cannot rule out the possibility that an endogenous F box protein similar to but distinct from β-TRCP may be involved in the Xom degradation.

β-TRCP is involved in several important degradation processes, such as β-catenin and IKBα in vertebrates (Kitagawa et al., 1999; Yaron et al., 1998), Cubitus interruptus (Ci) in *Drosophila* (Jiang and Struhl, 1998), as well as the human HIV-1 protein Vpu/CD4 (Maniatis, 1999; Margottin et al., 1998). Given these diverse targets, a key question is what gives specificity to these processes. In the case of β-catenin, local inhibition of GSK3 activity by the protein disheveled controls β-catenin degradation, presumably in a compartmentalized way; it is intriguing to think that proximity effects may also play a role in Xom degradation.

Regulated Proteolysis and Dorsoventral Pattern Formation in Early Gastrulation

The patterning of early gastrula mesoderm sets aside a BMP-free zone on the dorsal side. This has been explained by the expression of BMP inhibitors secreted by the Spemann organizer. We report here on another important process in dorsoventral patterning, which we feel contributes critically to the segregation of BMP signals to the ventral side. Nondegradable Xom is roughly 20 times more active than wild-type Xom in inhibiting the transcriptional activation of the Goosecoid promoter by activin and in blocking dorsoanterior development. This effect of stable Xom suggests that proteolysis of Xom is a required regulatory event terminating the inhibition of the expression of dorsal-specific genes on the dorsal side. Just after the midblastula transition, BMP4 and Xom are expressed throughout the embryo. Transcription of Xom is enhanced by BMP4. Xom expression in turn reinforces the expression of BMP4 in a potential autoactivating feedback loop that would maintain high BMP4 levels and block development of dorsal structures (Ladher et al., 1996; Onichtchouk et al., 1996). Something, therefore, is needed to break this loop.

As shown in Figure 7, our data suggest that regulated proteolysis of Xom at a specific time is essential for generating a dorsoventral pattern in the mesoderm during gastrulation. The proteolysis of Xom shows precise temporal regulation. At stage 10, there seems to be a slight bias causing more rapid loss of Xom on the dorsal relative to the ventral side (Figures 1D and 3D), but this in itself is probably not very important and may not be

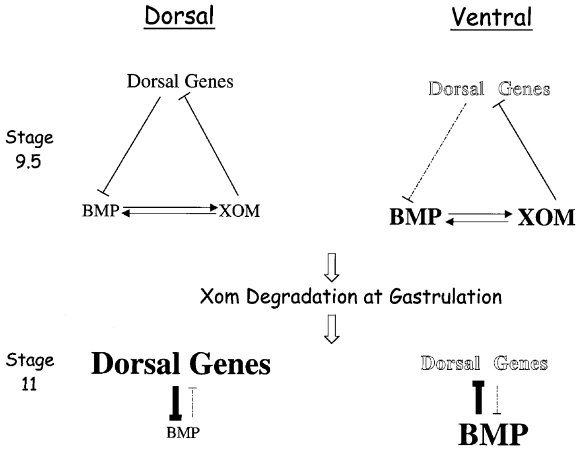

Figure 7. The Role of Xom Proteolysis in Dorsoventral Pattern Formation

In this model, the temporal degradation of Xom throughout the embryo is used to convert a bias in BMP distribution into an all or none process leading to distinct dorsoventral patterning. We assume that there will be other features of the circuit that also contribute but are not shown here. The elements of the circuit are very simple and are portrayed in four different states: dorsal at pregastrula (stage 9.5), dorsal at late gastrula (stage 11), ventral at pregastrula (stage 9.5), and ventral at late gastrula (stage 11). The circuit involves an activation of Xom by BMP and activation of BMP by Xom. Although this is transcriptional, the names signify protein activities. A second feature of the circuit is the inhibition of dorsal genes by Xom (transcriptional) and the inhibition of BMP *activity* by dorsal genes, such as *chordin*. At stage 9.5, there is a small excess of BMP on the ventral side, so that the BMP-Xom autoactivated circuit is shown in larger and bolder letters than the corresponding circuit on the dorsal side. This is due to the expression of BMP inhibitors on the dorsal side. By stage 11, Xom is degraded in both regions, eliminating the Xom-BMP autoactivating circuit. In the absence of dorsal genes on the ventral side, BMP activity remains high. Without the Xom-BMP autoactivating circuit, BMP activity declines to zero on the dorsal side. The result is large quantitative differences in BMP level and activity and dorsal gene expression in the two regions.

found in all embryos. What is clear and reproducible is the precise loss of Xom in the late gastrula. How does a signal that is not spatially localized contribute to spatial patterning? The high level of BMP4 on the ventral side must be self-maintaining in the absence of Xom. On the dorsal side, in the presence of BMP inhibitors, BMP4 is not self-maintaining when Xom is degraded. It is for this reason that Xom degradation has consequences on the dorsal side but no consequences on the ventral side. In this system, dorsoventral asymmetry in the mesoderm seems to be highly poised, set to collapse into either of two states: dorsal with low BMP4 and ventral with high BMP4; the reaction pathway will not allow intermediate states. As shown by Onichtchouk et al. (1996), this autoactivation loop can be easily broken by expressing a dominant-negative form of Xom. Physiologically, this loop is probably broken by secreted inhibitors of BMP4, which creates the initial dorsoventral bias, followed by the degradation of Xom. Smurf1 may also contribute to setting the dorsoventral threshold of BMP4 autoactivation. Together with recent findings that smurf1 mediates degradation of Smad1 and reduces BMP signaling (Podos et al., 2001; Zhu et al., 1999), we propose that temporally regulated proteolysis (and not necessarily spatially regulated proteolysis) may play a central regulatory role in embryonic patterning, converting a slight bias in BMP signaling into an all or none effect. There are two important unanswered questions related to the regulated degradation of Xom: how is Xom transiently stabilized in the early gastrulation stage and what turns on global Xom degradation later in gastrulation? Answering these questions will be required to understand the complex process of dorsoventral pattern formation during early development.

Experimental Procedures

Preparation of *Xenopus* Embryos and Embryonic Extracts

Xenopus embryos were obtained by in vitro fertilization. Embryos were cultured to specific stages as described (Kay and Peng, 1991) and staged according to the method of Nieuwkoop and Faber (1994). Embryonic extracts were prepared essentially as described, with some modifications (Salic et al., 2000). Embryos of specific developmental stages were collected and dejellied. After three washes with 0.1× Marc's Modified Ringer's (MMR) solution, the embryos were washed once in extraction buffer (XB; 100 mM KCl, 1 mM $MgCl_2$, 0.1 mM $CaCl_2$) with 100 mM sucrose and packed in 1.5 ml Eppendorf tubes by spinning at 300 g for 30 s. The embryos were then crushed at 21,000 g for 5 min. The cytoplasmic layer was removed and supplemented with 2 μl cytochalasin B (10 mg/ml in DMSO) and 1 μl of protease inhibitors (10 mg/ml of leupeptin, chemostatin, and pepstain in DMSO). The crude extracts were cleared by spinning at 21,000 g for 5 min twice. Energy mix (150 mM creatine phosphate, 20 mM ATP, 2 mM EDTA [pH 7.7], 20 mM $MgCl_2$) and ubiquitin (15 mg/ml) were added after the final spin, and aliquots of the staged extracts were quickly frozen in liquid nitrogen and kept in −80°C for further use. High-speed extracts were prepared as described (King et al., 1995) and used in the in vitro ubiquitination assay. Microinjection of RNA and DNA was carried out in 0.1× MMR containing 4% ficoll. After injection, embryos were transferred to a medium of 0.1× MMR and cultured to specific stages at a temperature below 19°C.

In Vitro Degradation Assay and Developmental Screen

Detailed methods for the in vitro degradation assay and screening of small pools of *Xenopus* cDNA libraries have been described (Lustig et al., 1997; Salic et al., 2000). In brief, [^{35}S]methionine-labeled proteins were obtained by transcription and translation coupling reactions of small pools of cDNAs using a Promega TNT kit (per the manufacturer's instructions). For a typical reaction, 0.5 μl of [^{35}S]methionine-labeled proteins were incubated with 4.5 μl of staged extracts supplemented with energy mix, ubiquitin, and cycloheximide at 22°C for 3 hr. Reactions were stopped by the addition of 2× sample buffer, and samples were analyzed by SDS-PAGE followed by autoradiography.

Ubiquitination Assay

Xom was labeled with [^{35}S]methionine in a TNT reaction. [^{35}S]methionine-labeled proteins (2 μl) were incubated with 20 μl high-speed extract supplemented with either regular ubiquitin or his_6-tagged ubiquitin (0.2 mg/ml) together with energy mix, protease inhibitors, and cycloheximide at room temperature for 1 hr. Following the reaction, the mixture was diluted 10-fold with PBS and 1% Tween-20 (pH 7.3), and 5 μl of Ni beads was added to the reaction. Binding was performed at 4°C for 2 hr. Bound materials were spun down briefly. After four washes with 0.5 ml of PBS, 1% Tween 20, the bound proteins were eluted with sample buffer and analyzed by SDS-PAGE and autoradiography.

In Vivo Xom Stability Assay

mRNA (0.4 ng) encoding myc-tagged Xom or Xom mutants was injected into two blastomeres at the two- to four-cell stage together with an internal marker of 0.1 ng myc-tagged GFP. For a typical reaction, five embryos were cultured to different developmental stages and collected in 1.5 ml Eppendorf tubes. The embryos were submerged in 50 μl XB and homogenized by pipetting up and down several times. The cytoplasm was cleared by brief spinning in the microcentrifuge at top speed; 5 μl of the clear extract was mixed with the same volume of 2× sample buffer and subjected to SDS-PAGE. The amount of Xom or Xom mutants was measured by Western blot with antibodies to myc.

Plasmids and Mutant Construction

Plasmids encoding F box proteins are generous gifts of Dr. Michele Pagano of the New York University Medical Center and Dr. Wade Harper of Baylor Medical College. Reagents for the luciferase assay were contributed by Dr. Malcolm Whitman of Harvard Medical School. Deletion mutations of Xom were made by PCR-based mutagenesis. Point mutations were created with the Stratagene QuickChange mutagenesis kit, according to the manufacturer's instructions. Primer sequences for mutagenesis will be provided upon request. All cDNAs were cloned in the CS2 plasmid and tested by sequencing and in vitro translation assay.

Luciferase Assay

For the luciferase assay, both blastomeres at the two-cell stage were injected with 10 nl of RNA encoding Xom or Xom mutants, together with 50 pg of activin RNA and 100 pg reporter plasmid. The embryos were cultured to stage 10–10.5. Five embryos were collected and lysed in 50 μl lysis buffer (Promega). After being microcentrifuged at top speed for 10 min at room temperature, luciferase activity was determined in 5 μl of the supernatant, according to the manufacturer's instructions and quantified with a scintillation counter.

In Vitro Binding Assay

Twenty amino acid peptides corresponding to the Xom destruction motif (residues 131–150) were synthesized in both wild-type form and with serines 140 and 144 doubly phosphorylated (with premade phosphoserine), and were coupled to agarose beads at 1 mg/ml (Genemed). To test the binding of the SCF/Skp1 complex with the destruction motif, staged extracts were diluted five times with XB, 0.1% NP-40, and protease inhibitors, and 10 μl of either phosphorylated peptide beads or control nonphosphorylated beads was added to 200 μl of the diluted extracts. After incubation at 4°C for 4 hr, beads were washed three times with binding buffer, and bound proteins were eluted with 50 μl sample buffer; 10 μl of the samples was subjected to SDS-PAGE and analyzed by Western blot using a monoclonal antibody to Skp1 and ECL reagent (Amersham).

Acknowledgments

We would like to thank Ethan Lee, Adrian Salic, Henry Ho, and other members of the Kirschner lab for technical support. We are grateful to Wade Harper, Michele Pagano, and Malcolm Whitman for providing critical reagents. We would like to thank Malcolm Whitman, Robert Davis, Jeffrey Peterson, and Licio Collavin for critical discussion of the experiments and comments on the manuscript. The project was supported by NIH grant R01HD37277-04. Zhenglun Zhu was supported by NIH grant T32DK07191, a Howard Hughes Physician Fellowship award, and is currently supported by an NIH NIDDK K08 award.

Received: February 12, 2002
Revised: July 26, 2002

References

Chen, Y., Gallaher, N., Goodman, R.H., and Smolik, S.M. (1998). Protein kinase A directly regulates the activity and proteolysis of cubitus interruptus. Proc. Natl. Acad. Sci. USA *95*, 2349–2354.

De Robertis, E.M., Larrain, J., Oelgeschlager, M., and Wessely, O. (2000). The establishment of Spemann's organizer and patterning of the vertebrate embryo. Nat. Rev. Genet. *1*, 171–181.

Deshaies, R.J., and Ferrell, J.E. (2001). Multisite phosphorylation and the countdown to S phase. Cell *107*, 819–822.

Fenteany, G., Standaert, R.F., Lane, W.S., Choi, S., Corey, E.J., and Schreiber, S.L. (1995). Inhibition of proteasome activities and subunit-specific amino-terminal threonine modification by lactacystin. Science *268*, 726–731.

Graff, J.M. (1997). Embryonic patterning: to BMP or not to BMP, that is the question. Cell *89*, 171–174.

Graff, J.M., Thies, R.S., Song, J.J., Celeste, A.J., and Melton, D.A. (1994). Studies with a *Xenopus* BMP receptor suggest that ventral mesoderm-inducing signals override dorsal signals in vivo. Cell *79*, 169–179.

Harland, R., and Gerhart, J. (1997). Formation and function of Spemann's organizer. Annu. Rev. Cell Dev. Biol. *13*, 611–667.

Hershko, A., and Ciechanover, A. (1998). The ubiquitin system. Annu. Rev. Biochem. *67*, 425–479.

Hochstrasser, M. (1996). Ubiquitin-dependent protein degradation. Annu. Rev. Genet. *30*, 405–439.

Hoppler, S., and Moon, R.T. (1998). BMP-2/-4 and Wnt-8 cooperatively pattern the *Xenopus* mesoderm. Mech. Dev. *71*, 119–129.

Howe, J.A., and Newport, J.W. (1996). A developmental timer regulates degradation of cyclin E1 at the midblastula transition during *Xenopus* embryogenesis. Proc. Natl. Acad. Sci. USA *93*, 2060–2064.

Jiang, J., and Struhl, G. (1998). Regulation of the Hedgehog and Wingless signalling pathways by the F-box/WD40-repeat protein Slimb. Nature *391*, 493–496.

Kao, K.R., and Elinson, R.P. (1988). The entire mesodermal mantle behaves as Spemann's organizer in dorsoanterior enhanced *Xenopus laevis* embryos. Dev. Biol. *127*, 64–77.

Kay, B.K., and Peng, H.B. (1991). *Xenopus Laevis*: Practical Uses in Cell and Molecular Biology, Volume 36, E.L. Wilsom, ed. (San Diego, CA: Academic Press).

King, R.W., Peters, J.M., Tugendreich, S., Rolfe, M., Hieter, P., and Kirschner, M.W. (1995). A 20S complex containing CDC27 and CDC16 catalyzes the mitosis-specific conjugation of ubiquitin to cyclin B. Cell *81*, 279–288.

Kirschner, M. (1999). Intracellular proteolysis. Trends Biochem. Sci. *24*, M42–M45.

Kitagawa, M., Hatakeyama, S., Shirane, M., Matsumoto, M., Ishida, N., Hattori, K., Nakamichi, I., Kikuchi, A., and Nakayama, K. (1999). An F-box protein, FWD1, mediates ubiquitin-dependent proteolysis of β-catenin. EMBO J. *18*, 2401–2410.

Klein, P.S., and Melton, D.A. (1996). A molecular mechanism for the effect of lithium on development. Proc. Natl. Acad. Sci. USA *93*, 8455–8459.

Ladher, R., Mohun, T.J., Smith, J.C., and Snape, A.M. (1996). Xom: a *Xenopus* homeobox gene that mediates the early effects of BMP-4. Development *122*, 2385–2394.

Laney, J.D., and Hochstrasser, M. (1999). Substrate targeting in the ubiquitin system. Cell *97*, 427–430.

Lanker, S., Valdivieso, M.H., and Wittenberg, C. (1996). Rapid degradation of the G1 cyclin Cln2 induced by CDK-dependent phosphorylation. Science *271*, 1597–1601.

Larabell, C.A., Torres, M., Rowning, B.A., Yost, C., Miller, J.R., Wu, M., Kimelman, D., and Moon, R.T. (1997). Establishment of the dorsoventral axis in *Xenopus* embryos is presaged by early asymmetries in β-catenin that are modulated by the Wnt signaling pathway. J. Cell Biol. *136*, 1123–1136.

Liu, C., Kato, Y., Zhang, Z., Do, V.M., Yankner, B.A., and He, X. (1999). β-Trcp couples β-catenin phosphorylation-degradation and regulates *Xenopus* axis formation. Proc. Natl. Acad. Sci. USA *96*, 6273–6278.

Lustig, K.D., Stukenberg, P.T., McGarry, T.J., King, R.W., Cryns, V.L., Mead, P.E., Zon, L.I., Yuan, J., and Kirschner, M.W. (1997). Small pool expression screening: identification of genes involved in cell cycle control, apoptosis, and early development. Methods Enzymol. *283*, 83–99.

Maniatis, T. (1999). A ubiquitin ligase complex essential for the NF-κB, Wnt/Wingless, and Hedgehog signaling pathways. Genes Dev. *13*, 505–510.

Margottin, F., Bour, S.P., Durand, H., Selig, L., Benichou, S., Richard, V., Thomas, D., Strebel, K., and Benarous, R. (1998). A novel human WD protein, h-β TrCp, that interacts with HIV-1 Vpu connects CD4 to the ER degradation pathway through an F-box motif. Mol. Cell *1*, 565–574.

McGarry, T.J., and Kirschner, M.W. (1998). Geminin, an inhibitor of DNA replication, is degraded during mitosis. Cell *93*, 1043–1053.

Miller, J.R., Rowning, B.A., Larabell, C.A., Yang-Snyder, J.A., Bates, R.L., and Moon, R.T. (1999). Establishment of the dorsal-ventral axis in *Xenopus* embryos coincides with the dorsal enrichment of dishevelled that is dependent on cortical rotation. J. Cell Biol. *146*, 427–437.

Murray, A. (1991). Cell cycle extracts. Methods Cell Biol. *36*, 581–605.

Nash, P., Tang, X., Orlicky, S., Chen, Q., Gertler, F.B., Mendenhall, M.D., Sicheri, F., Pawson, T., and Tyers, M. (2001). Multisite phosphorylation of a CDK inhibitor sets a threshold for the onset of DNA replication. Nature *414*, 514–521.

Newport, J., and Kirschner, M. (1982). A major developmental transition in early *Xenopus* embryos: I. characterization and timing of cellular changes at the midblastula stage. Cell *30*, 675–686.

Niehrs, C. (2001). The Spemann organizer and embryonic head induction. EMBO J. *20*, 631–637.

Nieuwkoop, P.D., and Faber, J. (1994). Normal table of *Xenopus laevis* (New York: Garland Publishing).

Onichtchouk, D., Gawantka, V., Dosch, R., Delius, H., Hirschfeld, K., Blumenstock, C., and Niehrs, C. (1996). The Xvent-2 homeobox gene is part of the BMP-4 signalling pathway controlling [correction of controlling] dorsoventral patterning of *Xenopus* mesoderm. Development *122*, 3045–3053.

Onichtchouk, D., Glinka, A., and Niehrs, C. (1998). Requirement for Xvent-1 and Xvent-2 gene function in dorsoventral patterning of *Xenopus* mesoderm. Development *125*, 1447–1456.

Papalopulu, N., and Kintner, C. (1996). A *Xenopus* gene, Xbr-1, defines a novel class of homeobox genes and is expressed in the dorsal ciliary margin of the eye. Dev. Biol. *174*, 104–114.

Paul, M., and Jabbar, M.A. (1997). Phosphorylation of both phosphoacceptor sites in the HIV-1 Vpu cytoplasmic domain is essential for Vpu-mediated ER degradation of CD4. Virology *232*, 207–216.

Peters, J.-M., Harris, J.R., and Finley, D. (1998). Ubiquitin and the Biology of the Cell (New York: Plenum Press).

Podos, S.D., Hanson, K.K., Wang, Y.C., and Ferguson, E.L. (2001). The DSmurf ubiquitin-protein ligase restricts BMP signaling spatially and temporally during *Drosophila* embryogenesis. Dev. Cell *1*, 567–578.

Salic, A., Lee, E., Mayer, L., and Kirschner, M.W. (2000). Control of β-catenin stability: reconstitution of the cytoplasmic steps of the wnt pathway in *Xenopus* egg extracts. Mol. Cell *5*, 523–532.

Schmidt, J.E., von Dassow, G., and Kimelman, D. (1996). Regulation of dorsal-ventral patterning: the ventralizing effects of the novel *Xenopus* homeobox gene Vox. Development *122*, 1711–1721.

Schubert, U., Henklein, P., Boldyreff, B., Wingender, E., Strebel, K., and Porstmann, T. (1994). The human immunodeficiency virus type 1 encoded Vpu protein is phosphorylated by casein kinase-2 (CK-2) at positions Ser52 and Ser56 within a predicted alpha-helix-turn-alpha-helix-motif. J. Mol. Biol. *236*, 16–25.

Skowyra, D., Craig, K.L., Tyers, M., Elledge, S.J., and Harper, J.W. (1997). F-box proteins are receptors that recruit phosphorylated substrates to the SCF ubiquitin-ligase complex. Cell *91*, 209–219.

Stukenberg, P.T., Lustig, K.D., McGarry, T.J., King, R.W., Kuang, J., and Kirschner, M.W. (1997). Systematic identification of mitotic phosphoproteins. Curr. Biol. *7*, 338–348.

Trindade, M., Tada, M., and Smith, J.C. (1999). DNA-binding specificity and embryological function of Xom (Xvent-2). Dev. Biol. *216*, 442–456.

Watabe, T., Kim, S., Candia, A., Rothbacher, U., Hashimoto, C., Inoue, K., and Cho, K.W. (1995). Molecular mechanisms of Spemann's organizer formation: conserved growth factor synergy between *Xenopus* and mouse. Genes Dev. *9*, 3038–3050.

Winston, J.T., Strack, P., Beer-Romero, P., Chu, C.Y., Elledge, S.J., and Harper, J.W. (1999). The SCFβ-TRCP-ubiquitin ligase complex associates specifically with phosphorylated destruction motifs in IκBα and β-catenin and stimulates IκBα ubiquitination in vitro. Genes Dev. *13*, 270–283.

Yaglom, J., Linskens, M.H., Sadis, S., Rubin, D.M., Futcher, B., and Finley, D. (1995). p34Cdc28-mediated control of Cln3 cyclin degradation. Mol. Cell. Biol. *15*, 731–741.

Yaron, A., Hatzubai, A., Davis, M., Lavon, I., Amit, S., Manning, A.M., Andersen, J.S., Mann, M., Mercurio, F., and Ben-Neriah, Y. (1998). Identification of the receptor component of the IκBα-ubiquitin ligase. Nature *396*, 590–594.

Yost, C., Torres, M., Miller, J.R., Huang, E., Kimelman, D., and Moon, R.T. (1996). The axis-inducing activity, stability, and subcellular distribution of β-catenin is regulated in *Xenopus* embryos by glycogen synthase kinase 3. Genes Dev. *10*, 1443–1454.

Zandi, E., Chen, Y., and Karin, M. (1998). Direct phosphorylation of IκB by IKKα and IKKβ: discrimination between free and NF-κB-bound substrate. Science *281*, 1360–1363.

Zhu, H., Kavsak, P., Abdollah, S., Wrana, J.L., and Thomsen, G.H. (1999). A SMAD ubiquitin ligase targets the BMP pathway and affects embryonic pattern formation. Nature *400*, 687–693.

Zou, H., McGarry, T.J., Bernal, T., and Kirschner, M.W. (1999). Identification of a vertebrate sister-chromatid separation inhibitor involved in transformation and tumorigenesis. Science *285*, 418–422.